

American Journal of Science

NOVEMBER 2007

THE RELATIONSHIP BETWEEN TECTONIC UPLIFT AND CHEMICAL WEATHERING RATES IN THE WASHINGTON CASCADES: FIELD MEASUREMENTS AND MODEL PREDICTIONS

MICHAEL T. HREN, GEORGE E. HILLEY, and C. PAGE CHAMBERLAIN

Department of Geological and Environmental Sciences, Stanford University,
Stanford, California 94305; hren@stanford.edu

ABSTRACT. Tectonic uplift is one of the key factors controlling the supply of material to weathering environments. At present however, there is debate about whether tectonics or climate plays a larger role in controlling chemical weathering rates on a global scale over geologic time. We measured riverine weathering fluxes from twelve catchments along the Skykomish River in the Washington Cascades, where long-term exhumation rates have been constrained by (U-Th)/He thermochronometry, to examine the effect of tectonic uplift on chemical weathering rates. We show that in the western Washington Cascades, dissolved Si fluxes increase from approximately 1900 to 3000 mol ha⁻¹ yr⁻¹ from west to east across the range and are correlated with rock exhumation rates. We use dissolved Si flux data from these catchments, depth to bedrock measurements, and long-term exhumation rates to test a steady-state weathering model that describes the relative importance of reaction kinetics and rock supply on weathering rates. Characterization of study basins with respect to two key variables in this model, weathering zone depth and exhumation rate, allows us to examine the relative effects of climate and tectonics on chemical weathering by analyzing the ratio of the timescale of reaction kinetics and the residence time in the weathering zone. Evaluation of this model shows that chemical weathering rates in the Cascades are controlled by the rate of rock erosion and factors that influence the depth of the active weathering zone. However, the model predicts that in tectonically inactive areas, the supply of material limits the overall rate of chemical weathering while in active tectonic or erosional environments, the rate of supply exceeds the ability of a system to weather that material resulting in a landscape in which weathering rates are expected to respond strongly to changes in climatic conditions.

INTRODUCTION

Tectonic uplift and climate are two key components in the global regulation of chemical weathering rates over geologic time (Berner and others, 1983). These parameters influence the rate of supply of rock to a landscape through rock erosion as well as the chemical processes in a weathering zone and the residence time of material within the weathering environment. As a result, on long timescales, chemical weathering rates may be strongly coupled to physical erosion rates and thus mountain uplift (Stallard and Edmond, 1983), and it has been argued that tectonic uplift of the earth's surface is the primary mechanism for regulating the intensity of global silicate weathering rates and the consumption of atmospheric CO₂ over time (Raymo and others, 1988; Raymo and Ruddiman, 1992).

In an effort to understand the relationship between tectonic uplift, erosion and chemical weathering, a number of recent studies have examined the effect of rock supply on chemical weathering rates (Riebe and others, 2001a; Jacobson and others 2003; Riebe and others, 2004a; Waldbauer and Chamberlain, 2005; Chamberlain and

others, 2005; West and others, 2005). These studies show that landscapes characterized by rapid erosion display high chemical weathering fluxes, primarily as a result of a strong coupling between physical and chemical erosion rates (Riebe and others, 2001b). This coupling between tectonics, erosion and chemical weathering is demonstrated in field studies (Riebe and others, 2001a, 2003, 2004a) and global compilations of riverine Si and base cation fluxes (Waldbauer and Chamberlain, 2005) and is supported by models that emphasize the role of tectonics in chemical weathering (West and others, 2005). Chemical weathering models and field data suggest that in steady-state weathering environments, chemical weathering rates should correlate strongly with physical erosion rates and only weakly with climate (Riebe and others, 2001a, 2004a) and weathering fluxes should be directly proportional to the rate of supply of weatherable material in regions limited by the rate of removal of material from a system (Waldbauer and Chamberlain, 2005; West and others, 2005).

To further explore the relationship between chemical weathering and rock uplift we examined dissolved riverine Si and base cation fluxes in the Washington Cascades. We chose this area to test predictions of a steady-state weathering model (Waldbauer and Chamberlain, 2005; Chamberlain and others, 2005) because recent measures of apatite (U-Th)/He ages provides a detailed record of the long-term exhumation history of the Washington Cascades range on a landscape scale (Reiners and others, 2002, 2003). The steady-state chemical weathering model of Waldbauer and Chamberlain (2005) predicts that chemical weathering should be coupled to long-term exhumation rates, which is observed in global compilations of dissolved riverine Si fluxes. However, whether this model applies to smaller-scale catchments is unknown. Therefore, we measured dissolved riverine Si fluxes from twelve catchments across climatic and tectonic gradients in the Skykomish River in the western Washington Cascades. This region is ideal for such a study because: 1) we can control for the effects of bedrock composition on weathering rates by sampling only catchments underlain by rocks of bulk granitic/granodioritic composition; 2) this drainage has a number of historic and actively gauged streams which allows us to convert Si concentrations to fluxes; 3) precipitation patterns and temperature gradients in this drainage system are reasonably well known; and 4) there is extensive information on rock exhumation for this area (Reiners and others, 2002, 2003). Our analysis of weathering fluxes from the Washington Cascades shows that as predicted by models of steady-state weathering (Waldbauer and Chamberlain, 2005) and weathering studies from mountainous areas with high erosion rates (Riebe and others, 2001a, 2001b, 2004b), Si fluxes correlate with long-term erosion rates and weakly or not at all with climatic variables.

METHODOLOGY

Criteria for Selection of Catchments Within the Skykomish River Drainage

We collected stream waters from twelve catchments in the Skykomish river drainage in the western Washington Cascades in 2003–2004 (fig. 1). These catchments were selected based on two criteria. First, the catchments were all underlain by rocks of primarily granitic or granodioritic composition. While the dominant bedrock type underlying the Skykomish River catchment consists of large Neogene plutons of primarily granodioritic composition, also found within this catchment are Paleozoic and Mesozoic sediments consisting largely of argillites and graywackes with lesser amounts of metamorphosed gabbros, marbles, and felsic volcanics (Tabor and Crowder, 1969; Tabor and others, 1993). We specifically avoided catchments with abundant marbles and gabbros. Second, we sampled catchments across the exhumation gradient as given by Reiners and others (2002, 2003). Apatite and zircon (U-Th)/He ages from plutons throughout the Skykomish catchment and across the western and central Cascades show that long-term (10^6 to 10^7 years) exhumation rates vary significantly

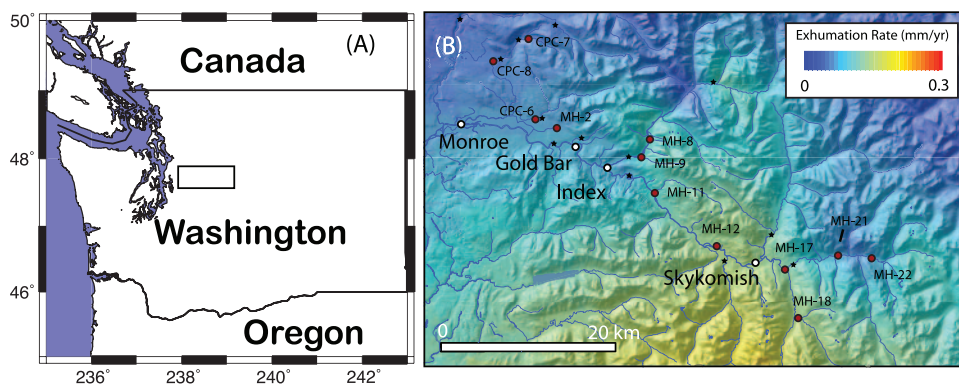


Fig. 1. Location map (A) of the Skykomish River in the central Washington Cascades. (B) Stream sample locations and extrapolated exhumation rate for the Skykomish River area.

within the orogen, with the highest exhumation rates occurring west of the crest of the Cascades (Reiners and others, 2002, 2003). We were able to sample across much of this exhumation gradient by selecting catchments near the crest of the Cascades and catchments well west of the crest.

Data Collection and Analysis

Water samples were collected at the edge of the stream channel in swift-flowing water four times from December 2003 to August 2004 at approximately 3-month intervals, to capture seasonal variations in solute concentrations during high and low flow conditions. Water samples were collected in acid washed HDPE vials and filtered with Whatman 0.45 μm filters. Stream pH was measured on site with an Accumet AP-61 pH meter and alkalinity measurements were made by Gran titration with HCl soon after sample collection. Accuracy of pH measurements is within ± 0.05 . We analyzed stream waters for Si and major cations on an inductively-coupled plasma atomic emission spectrometer at Stanford University. Anion data was collected on a Dionex Ion Chromatograph using an AS-4A SC column. Analytical uncertainty for these analyses is within ± 5 percent for all solute measurements. Sampling locations, timing, and solute data is given in table 1. Measures of the charge balance between total cations and anions in water samples (defined as $(\text{TZ}^+ - \text{TZ}^-)/(\text{TZ}^+ + \text{TZ}^-)$; where total dissolved cations $\text{TZ}^+ = \text{Na}^+ + \text{K}^+ + 2\text{Mg}^{2+} + 2\text{Ca}^{2+}$ and total dissolved anions $\text{TZ}^- = \text{Cl}^- + \text{NO}_3^- + 2\text{SO}_4^{2-} + \text{HCO}_3^-$) provides a means of evaluating the quality of chemical analyses. For most samples analyzed, the balance between total cationic and anionic charge is within 15 percent, which is close to the expected uncertainty for solute measurements.

Climatic Data for Individual Catchments

To examine the effect of climatic factors on chemical weathering rates, we generated mean annual precipitation and temperature grids for the Skykomish basin from monthly precipitation and temperature data available from the Spatial Climate Analysis Service, Oregon State University, and sampled to 1 km^2 . The maximum variability in precipitation over the study area ranges from less than 200 cm yr^{-1} in the lowest, westernmost portions of the basins, to nearly 350 cm yr^{-1} in areas of peak precipitation. For the catchments of interest, modeled basin mean precipitation ranges from 220 cm yr^{-1} to 265 cm yr^{-1} . It is important to note however, that in the Skykomish basin, monthly precipitation models show that peak precipitation does not

TABLE 1
Sampling locations, dates, and solute concentrations

Site	Sampling Date	River	pH	3 Month Discharge (L)	Ca ²⁺	K ⁺	Mg ²⁺	Na ⁺	Si	Cl ⁻	NO ₃ ⁻	SO ₄ ²⁻	HCO ₃ ⁻	TDS
					(μmol/L)									
CPC-6	12/14/03	Wallace Creek	6.81	3.18E+10	105	14	22	59	104	14	15	27	222	27
	2/29/04		6.73	3.21E+10	107	8	25	57	109	78	10	22	213	28
	6/4/04		7.00	4.44E+10	27	1	5	12	45	19	5	17	179	16
	8/6/04		6.75	1.20E+10	137	11	28	64	93	29	<i>B.D.</i>	24	267	30
CPC-7	12/14/03	Olney Creek	6.75	8.66E+09	130	6	20	41	69	-	-	-	-	-
	2/29/04		6.90	1.07E+10	179	18	31	91	81	107	<i>B.D.</i>	26	404	44
	6/4/04		6.80	1.12E+10	134	1	20	38	71	11	3	20	259	27
	8/6/04		6.86	3.27E+09	201	8	31	58	67	23	<i>B.D.</i>	22	477	44
CPC-8	12/14/03	Olney Creek	6.74	1.96E+10	120	7	27	53	81	-	-	-	-	-
	2/29/04		7.09	2.13E+10	129	6	29	53	82	54	7	27	268	31
	6/4/04		6.86	2.66E+10	124	3	26	47	79	21	<i>B.D.</i>	22	259	28
	8/6/04		6.84	7.41E+09	180	12	42	77	88	31	11	30	355	39
MH-2	12/14/03	Hogarty Creek	7.20	1.37E+10	50	10	14	43	89	-	-	-	-	-
	2/29/04		6.90	1.16E+10	46	12	13	43	89	17	10	20	80	14
	6/4/04		6.85	1.53E+10	40	9	12	38	77	10	6	15	77	12
	8/6/04		6.75	4.38E+09	55	11	16	50	99	16	7	15	128	17
MH-8	12/14/03	Bitter Creek	7.15	2.81E+09	51	42	11	155	106	-	-	-	-	-
	2/29/04		7.23	4.12E+09	47	10	11	41	96	46	6	10	103	15
	6/4/04		7.00	3.40E+09	26	4	5	23	55	7	1	5	59	8
	8/6/04		6.65	1.06E+09	37	7	7	31	52	35	<i>B.D.</i>	8	89	12
MH-9	2/29/04	Lewis Creek	6.26	5.22E+09	48	12	19	42	104	79	<i>B.D.</i>	20	59	15
	6/4/04		6.41	4.57E+09	41	7	14	29	74	10	<i>B.D.</i>	14	87	12
	8/6/04		6.27	1.41E+09	45	10	16	32	73	23	<i>B.D.</i>	20	113	15
	12/14/03		-	3.75E+09	-	-	-	-	-	-	-	-	-	-
MH-11	12/14/03	Barclay Creek	6.30	1.45E+10	42	9	28	37	107	-	-	-	-	-
	2/29/04		6.28	1.66E+10	45	10	33	41	115	14	9	19	116	17
	6/4/04		6.25	1.94E+10	35	7	20	32	87	10	3	12	79	12
	8/6/04		6.13	5.49E+09	51	11	39	42	37	15	<i>B.D.</i>	17	186	19
MH-12	12/14/03	Tributary of Money Creek	6.13	2.40E+11	71	7	18	49	135	-	-	-	-	-
	2/29/04		6.50	1.77E+11	55	7	16	53	138	28	<i>B.D.</i>	9	143	18
	6/4/04		6.69	3.75E+11	60	12	19	40	94	9	<i>B.D.</i>	9	138	16
	8/6/04		6.55	8.98E+10	89	18	27	66	101	24	<i>B.D.</i>	14	245	26
MH-17	12/14/03	S. Fork Foss River	6.57	9.35E+10	100	14	32	76	98	-	-	-	-	-
	2/29/04		7.00	7.98E+10	104	9	32	57	107	69	<i>B.D.</i>	10	245	28
	6/4/04		6.81	1.39E+11	59	5	17	33	72	5	<i>B.D.</i>	6	143	15
	8/6/04		7.01	3.51E+10	69	9	20	41	75	11	<i>B.D.</i>	5	169	18
MH-18	12/14/03	Tributary of Foss River	6.65	1.80E+09	86	6	44	53	103	107	<i>B.D.</i>	22	178	26
	2/29/04		7.29	2.83E+09	111	8	56	62	108	41	<i>B.D.</i>	26	303	33
	6/4/04		7.10	2.13E+09	82	5	37	53	107	11	<i>B.D.</i>	20	201	23
	8/6/04		7.09	6.82E+08	150	11	75	108	124	25	<i>B.D.</i>	40	451	46
MH-21	12/14/03	Skykomish River	6.50	1.11E+11	98	21	27	77	124	-	-	-	-	-
	2/29/04		6.58	9.23E+10	113	22	31	99	131	196	3	20	209	34
	6/4/04		6.97	1.66E+11	61	12	16	38	90	12	<i>B.D.</i>	8	140	16
	8/6/04		7.10	4.17E+10	116	26	30	107	121	45	<i>B.D.</i>	17	329	36
MH-22	12/14/03	Tye River	6.76	4.02E+10	56	16	13	40	85	20	1	9	130	16
	2/29/04		6.76	3.91E+10	111	31	25	148	133	47	3	22	293	35
	6/4/04		6.85	5.68E+10	60	6	17	32	82	5	<i>B.D.</i>	6	139	15
	8/6/04		7.10	1.51E+10	102	62	24	214	149	9	<i>B.D.</i>	25	379	42

correspond directly to elevation and the areas of highest precipitation lie to the west of the topographic crest of the Cascades.

Maximum and minimum mean annual temperatures over the areas of study range from 0°C at the highest peaks to approximately 10°C in the western portions of the watershed. The lowest mean annual temperatures occur in the regions of highest elevation. Mean annual basin temperatures range from 4 to 7°C for the study catchments and generally correspond with basin elevation. The climate data are given

in addition to atmospheric corrected Si and cation fluxes in table 2. Importantly, both precipitation and temperature data for the studied catchments are generated from spatial climate models sampled to 1 km². Because our catchments are generally small, downsampling climate models to 1 km² may introduce a degree of error to precipitation or temperature estimates for the smallest of our basins.

Catchment Discharge and Riverine Elemental Fluxes

Quantifying basin-wide chemical weathering rates from riverine solute concentrations requires estimates of total yearly stream discharge and accurate measures of stream water chemistry. In many instances, estimates of total water fluxes can be calculated from measurements of total annual precipitation or runoff. However, in areas where precipitation can be in the form of rain or snow, peak discharge does not always coincide with peak precipitation. We chose the Skykomish basin in the Washington Cascades to examine the role of climate and tectonic uplift on chemical weathering fluxes in part because there are a number of historic and actively gauged streams within this catchment that can be used to generate discharge/drainage area relationships to calculate stream discharge at each water sampling location.

The hydrograph for the Skykomish River shows that there are strong seasonal differences in discharge (fig. 2). Discharge peaks during the months of April to early June, and is generally at its lowest during the months of July to September. However, short-duration high discharge events are also evident in the stream hydrograph at other times of the year, such as in heavy rain periods in November. Using the stream hydrograph, we divided the year into four distinct periods of stream flow for water sampling: Jan–Mar, April–Jun, July–Sept, and Oct–Dec. We used records of daily discharge from twelve USGS stream gauging stations in the Skykomish basin that span a range of east-west locations, elevations and climatic regimes to calculate the mean stream discharge for each three-month period for the gauged stations. These three-month mean seasonal discharges were then used to calculate basin-wide discharge/drainage area curves for the Skykomish catchment. Using the catchment drainage area of each of our stream sample locations we calculated the seasonal mean, and three-month total river discharge for our water sampling sites. The three-month seasonal discharges used to generate flux measures are included in table 1. The R² value for the fit of these seasonal relationships are >0.90 for winter, spring, and summer periods and 0.86 for fall, which attests to the strength of this approach. USGS river gauging stations used in this calculation are shown in figure 1 and include: USGS 12130500 South Fork Skykomish River near Skykomish, Washington, USGS 12131000 Beckler River, USGS 12132000 Miller River, USGS 12133500 Troublesome Creek near Index, Washington, USGS 12134000 North Fork Skykomish at Index, Washington, USGS 12135000 Wallace River at Gold Bar, Washington, USGS 12135500 Olney Creek near Gold Bar, Washington, USGS 12136000 Olney Creek near Startup, Washington, USGS 12136500 May Creek near Gold Bar, Washington, USGS 12137290 South Fork Sultan River near Sultan, Washington, USGS 12137500 Sultan River near Startup, Washington, USGS 12129000 Tye River near Skykomish, Washington. We were unable to sample one location (MH-9) during the December 2003 sampling period due to inaccessibility and as a result, we used the mean solute concentrations of the other three sampling periods and the Oct–Dec discharge to estimate this seasonal and annual riverine weathering flux. This method is appropriate for this sampling location because at this site, stream waters exhibit little variability in solute concentrations throughout the three seasonal sampling periods.

Annual evapotranspiration in the Skykomish catchment may be as much as 350 mm yr⁻¹ (Tangborn and Rasmussen, 1976), which is greater than ten percent of total calculated 2003–2004 basin precipitation. However, calculated annual discharges produced from the discharge/drainage area relationships are approximately equal to

TABLE 2
Solute fluxes and basin characteristics

Site	Geology	Latitude (N)	Longitude (W)	km East ¹	Drainage Area (km ²)	Basin Elevation (m)	Basin avg. soil depth (m)	Long-term Erosion Rate (mm/yr)	Basin Mean Precipitation (2003-2004) (cm)	Basin Mean Temperature (°C)	Annual Flux (mol ha ⁻¹ y ⁻¹)						
											Si	Ca	Na	Mg	K	W _{chem} ²	W _{CO₂} ³
CPC6	Biotite Gneiss/ Sandstone/Shale	47.864	121.6816	94	48.5	814	0.40	0.08	237	6.9	2046	1961	892	416	181	5497	4092
CPC7	Granodiorite	47.946	121.6896	90	13.1	964	0.39	0.07	231	5.8	1891	3954	1350	631	209	8035	3782
CPC8	Granodiorite	47.924	121.7435	84	29.9	727	0.42	0.06	220	7.3	2039	3251	1207	711	139	7346	4079
MH2	Schist	47.854	121.6487	96	17.6	847	0.39	0.09	252	6.8	2194	1159	922	328	262	4865	4388
MH8	Granodiorite/ Biotite Gneiss	47.841	121.5072	107	4.2	1163	0.25	0.12	257	4.5	2232	1088	1551	229	419	5519	4463
MH9	Graywacke/Schist	47.823	121.5188	106	5.6	979	0.32	0.12	275	5.5	2455	1199	812	458	270	5194	4910
MH11	Graywacke/Schist/ Granodiorite	47.787	121.5014	108	22.1	1033	0.32	0.13	265	5.6	2426	1036	776	699	222	5159	4852
MH12	Granodiorite	47.73	121.4085	115	370.2	1132	0.35	0.13	235	5	2727	1535	996	442	241	5940	5453
MH17	Biotite Gneiss/ Feldspathic Sandstone/Shale	47.705	121.3051	122	143.5	1269	0.34	0.17	251	4.3	2111	1956	1079	584	200	5932	4223
MH18	Granodiorite	47.69	121.2961	123	2.7	1008	0.39	0.13	234	5.1	2967	2744	1559	1348	189	8807	5934
MH21	Biotite gneiss	47.718	121.2239	129	170.7	1286	0.35	0.11	229	4.1	2692	2108	1541	559	435	7335	5385
MH22	Granodiorite	47.715	121.1732	133	61.4	1275	0.34	0.10	221	4.2	2524	1872	1899	449	497	7241	5049

¹km East relative to a UTM Easting of 504645 as used in Reiners and others, 2003.

²W_{chem} = Si + Ca + Na + Mg + K.

³Using the relationship W_{CO₂} = 2Si_{Flux} (Edmonds and Huh, 1997).

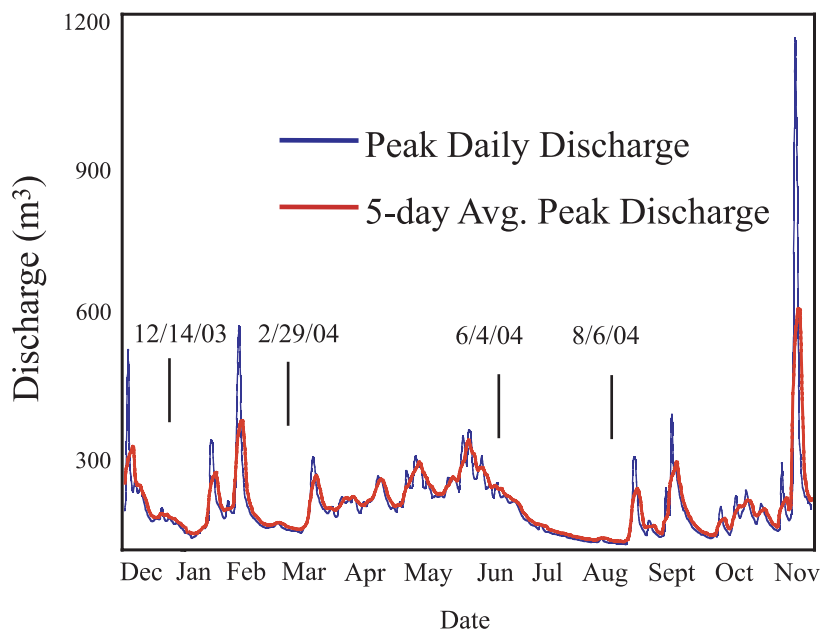


Fig. 2. Stream discharge (m^3) for the Skykomish river at Gold Bar, WA, during the 2003-2004 sampling period.

total annual precipitation estimates for each basin from PRISM climate models. The closeness of these values likely results from uncertainties in the downsampling of climatic data to the size of individual basins and in comparing precipitation models of 2003–2004 with stream discharges calculated from long-term discharge/drainage area relationships. Despite this, the maximum variability in long-term (1928–2004) annual discharge of the Skykomish River at Gold Bar, Washington is 22 percent. Thus, it may be reasonable to assume that error in calculated annual discharge for each location is likely not greater than the maximum variability observed in annual discharge over the past 76 years of record.

Depth to Bedrock

To examine whether chemical fluxes exhibit any correlation with the mean depth to bedrock within a given catchment and to test a steady-state weathering model that requires estimates of weathering zone depths (Waldbauer and Chamberlain, 2005), we measured the depth to bedrock at 225 locations throughout the Skykomish basin. The goal of this measurement was to develop a reasonable, if imperfect, measure of the depth of the zone from which chemical weathering products are derived. While the depth of the zone of active rock weathering may extend several meters below the rock/soil interface and the weathering of rock below the layer of soil colluvium can contribute a significant percentage of all dissolved ions for some bedrock types (White and others, 1998; Anderson and others, 2002), much of the chemical weathering in terrain underlain by graywacke has been shown to occur in the soil and saprolite (Anderson and others, 2002). In addition, weathering studies at Rio Icosos, Puerto Rico, show that a significant portion of weathering occurs in a shallow zone near the saprolite/rock interface (White and others, 1998). Thus, the depth to bedrock provides a relative measure of the thickness of the zone in which the bulk of rock weathering occurs, and is more readily quantifiable across a catchment than the total

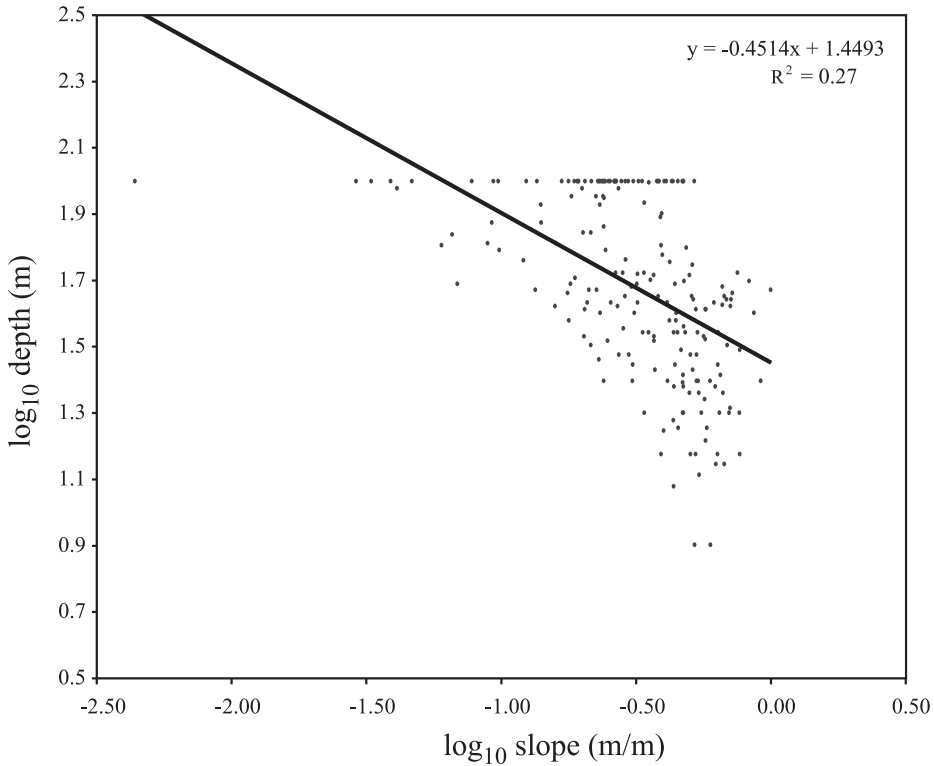


Fig. 3. Depth to bedrock as a function of local slope. Measurements from 225 sampling locations were used to generate estimates of landscape depths to bedrock.

depth of the zone of leaching. As such, depth to bedrock measurements in this study include soil colluvium and saprolite where present, but do not include regolith. To assess basin-wide depth to bedrock, measurements were taken from valley sides and bottoms, forested hill slopes and steep mountain sides and were made from soil pits, soil cores or exposed soil-rock surfaces at road cuts or landslides. Because of difficulties in accessing the steep-sloped areas of open rock faces and mountaintops, our soil depth dataset does not include any zero depth measurements. Using Digital Elevation Models we compared measured depth to bedrock with hillslope angle, surface curvature, and elevation in an attempt to extrapolate depth over the landscape.

Although previous studies have shown soil depth to correlate with hillslope curvature (Heimsath and others, 1997), in this catchment, depth to bedrock showed the strongest relationship with local hillslope angle. This may result from a lack of detailed hillslope curvature data due to the 30 m resolution of our Digital Elevation Models. As a result, the relationship between the log of local slope and depth to bedrock was used to determine the weathering zone depth across a catchment (fig. 3). Depths from each 30 by 30 m portion of a catchment were then used to generate catchment mean depth to bedrock measures. Modeled basin mean depth to bedrock ranges from 25 to 40 cm throughout the analyzed catchments (table 2) and is correlated with basin mean temperature, precipitation, and exhumation rate. Depths decrease with increasing basin elevation and cold temperatures, and are greater in basins with low rates of long-term exhumation and higher precipitation (fig. 4).

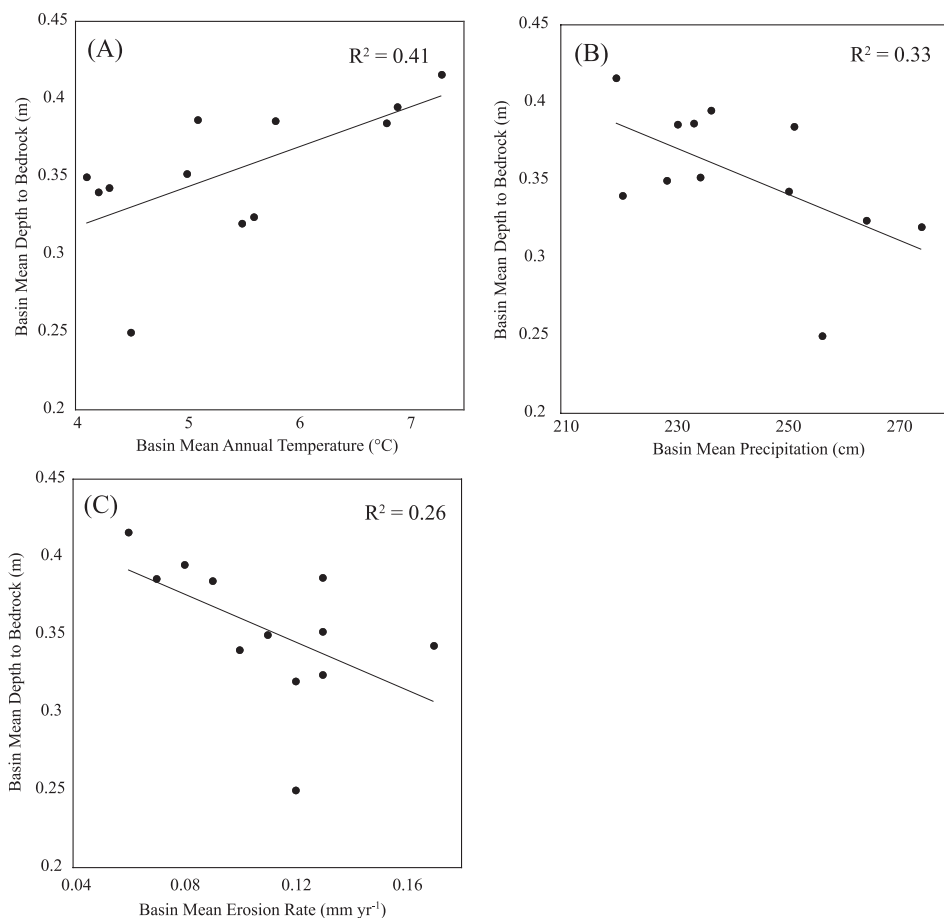


Fig. 4. Calculated basin mean depth to bedrock against (A) basin mean temperature, (B) basin mean annual precipitation (cm), and (C) basin mean exhumation/erosion rate. Depth is most strongly correlated with temperature and basins with higher mean annual temperatures are characterized by greater thicknesses of soil colluvium and saprolite.

One difficulty in generating reasonable estimates of depth to bedrock throughout our catchments is that in some areas of the Cascades, the layer of soil colluvium and saprolite may be much deeper than several meters (Anderson and others, 2002). In the absence of obtaining drill cores throughout the catchment, it is difficult to quantitatively characterize areas where soils are significantly greater than 1 m depth. As such, our model of depth to bedrock across the landscape may be biased towards underestimation of the basin average depth to bedrock. Indeed, we were unable to measure the full depth to bedrock in areas where this exceeded 1 m, which comprised roughly 20 percent of our measurements. However, as seen in the broad relationship between the log of the depth to bedrock and local slope (fig. 3), most of the regions with depths 1 m or greater are areas with low slope, such as valley sides and floodplain areas.

Although our measures of basin average depth to bedrock may systematically underestimate the true depth of zones from which all chemical fluxes are derived, it is likely that the measures of mean basin depth to bedrock for the twelve catchments are reasonable estimates for several reasons. First, most of the Skykomish basin is character-

ized by steep slopes, thin soils, and minimal or thin saprolite (<80 cm). Second, steep sloped areas comprise the largest percentage of areas in the studied catchments. In our calculated model of depths, depth to bedrock ranges from 0 to 2.5 m over the land surface and predictably decreases on high elevation, steep sloped surfaces, and reaches maximum depth on valley bottoms. Third, our modeled depths are in good agreement with depth to bedrock measures for Skykomish, Marblemount, and Blethen series soils (65 – 115 cm) for the Skykomish area (Soil Survey Report of Snohomish County, 1983). They are also similar, though generally lower, than studies from a small catchment underlain by graywacke in the southern Cascades that has a mean soil colluvium depth of 0.7 m and overlies saprolite with an average thickness of 0.23 m (Anderson and others, 2002). Our depth estimates are lower than these because our study area is underlain primarily by less easily weathered granodiorite bedrock, has lower mean annual temperatures, and many of our catchments have large areas (km²) of exposed bedrock with modeled depths of 0, all of which support relatively low mean depth to bedrock in our basins. Thus, while we acknowledge that the error in the depth to bedrock model at any point in the landscape may be large, particularly in valley bottoms, when averaged over the area of study, errors in these measurements are reduced and basin average depth to bedrock estimates are likely reasonable characterizations of relative differences in depth to bedrock in the studied catchments.

Long-Term Catchment Exhumation Rates

To examine the relationship between long-term tectonic uplift/exhumation and chemical weathering, we calculated landscape-wide long-term exhumation/erosion rates from published apatite (U-Th)/He data (Reiners and others, 2002, 2003) using the methods outlined in Brandon and others (1998) and Reiners and others (2003). We extrapolated calculated point erosion rate measurements across the length and width of the Cascades using a kriging algorithm with a spherical model variogram to construct a map of long-term erosion rates in the area. Thus, with the assumption of steady-state the inferred exhumation rate may be equated with rock uplift rate (U) at each point in the Skykomish watershed. Calculated long-term exhumation rates range from 0.05 to 0.33 mm yr⁻¹ over the Cascade range near the Skykomish basin (fig. 1; Reiners and others, 2003), however average rates of exhumation for each of the twelve studied catchments range from 0.06 to 0.17 mm yr⁻¹ (table 2; fig. 5A). Potential uncertainty in calculated exhumation rates is derived from uncertainty in geothermal gradients, apatite (U-Th)/He measurements, and topographic effects on bending isotherms. As reported by Reiners and others (2003), maximum error in spot exhumation rates from topographic effects is 9 to 14 percent. Uncertainty in these measures is compounded by error in the geothermal gradient for very young (U-Th)/He ages (Reiners and others, 2003), and extrapolation of spot exhumation rates across our catchment.

RESULTS

Solute Data

Stream waters from the Skykomish catchments contain relatively dilute concentrations of base cations and anions. In general, the Total Dissolved Solids (TDS = Ca²⁺ + Mg²⁺ + K⁺ + Na⁺ + Si + Cl⁻ + NO₃⁻ + SO₄²⁻ + HCO₃⁻) for these streams range from 8 mg L⁻¹ to 44 mg L⁻¹. The pH of most streams are generally circumneutral, although several sample sites have relatively low pH, from 6.1 to 6.4. Streams show a range of variability in water pH throughout the year, and some sampling locations show up to 0.5 to 0.6 pH unit differences between seasonal sampling periods. However, no clear trend is observed in seasonal pH in these samples (table 1).

In general, Ca²⁺ is the dominant cation in the tributaries along the Skykomish, contributing nearly 50 percent of cations on a molar basis. Na⁺ is the next most

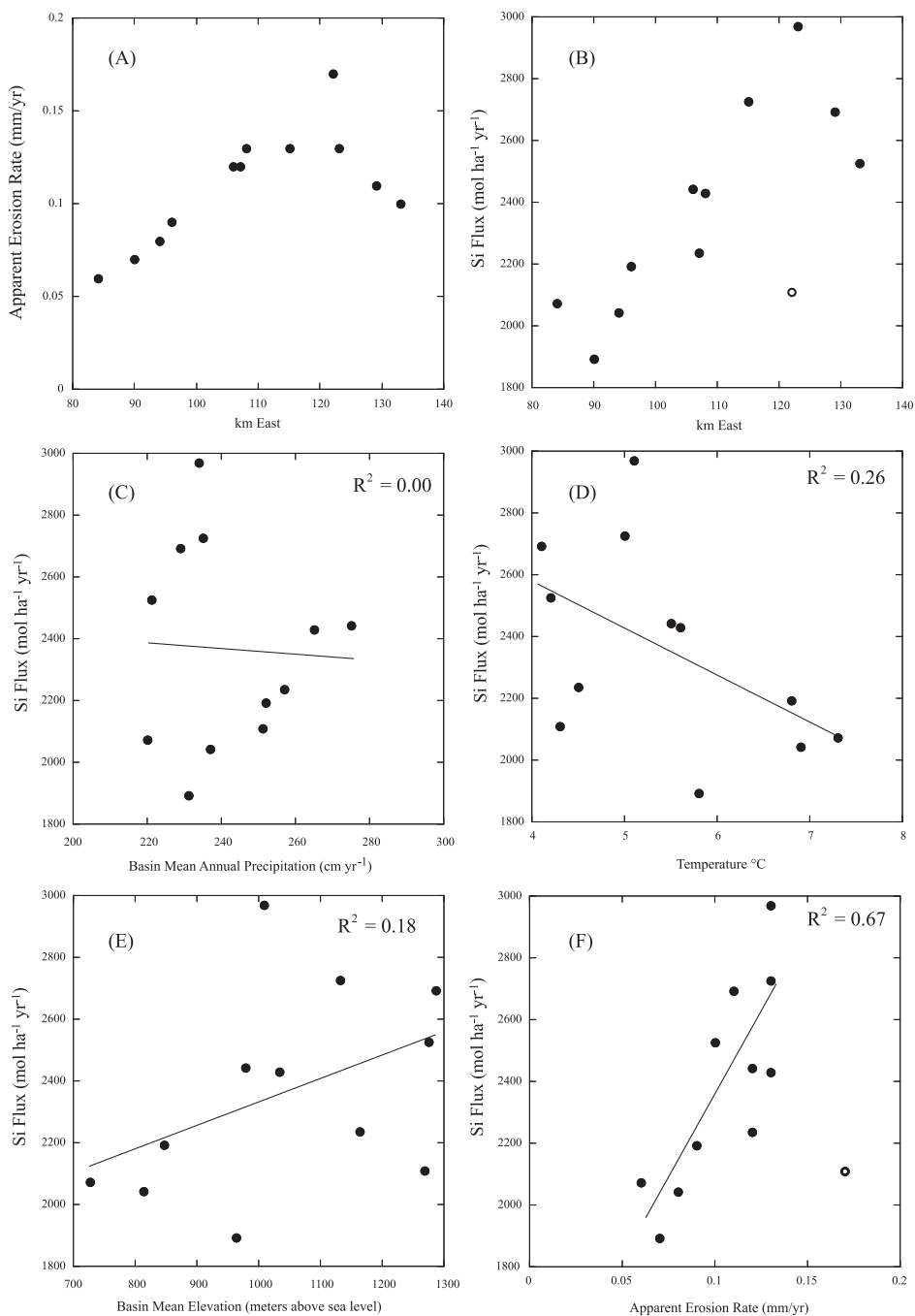


Fig. 5. Apparent exhumation/erosion rate and Si flux against a range of environmental parameters. Plot (A) shows basin average erosion rate as a function of east-west position relative to a UTM of 504645. Plots B through F show Si fluxes as a function of basin east-west position, basin-averaged precipitation, temperature, elevation, and exhumation/erosion rate with best fit lines and R² values.

abundant (30%), followed by Mg^{2+} (15%) and K^+ (5%). HCO_3^- is the most common anion in the streams analyzed, comprising on average more than 75 percent of total anions on a molar basis in stream samples. Cl^- and SO_4^{2-} also make up significant portions of the total anionic contribution (15% and 7%, respectively) and NO_3^- comprises only a minor portion of total anions.

In some systems, variations in solute concentrations with discharge can impart a significant degree of uncertainty in annual flux estimates because solute concentrations at any point in time may not necessarily reflect long-term average concentrations or the concentrations of solutes during peak discharge events. This is particularly important in basins characterized by “spikiness” in discharge records. Measured variations in solute concentrations are smallest for Si, and considerably larger for other major ions. In general, the variations in dissolved Si concentration are less than 50 to 60 percent between peak and minimum concentrations, 100 percent for Ca^{2+} , 140 percent for Na^+ , 115 percent for Mg^{2+} , and 200 to 300 percent for K^+ . These variations in solute concentrations of Cascades rivers likely result from seasonal changes in the proportion of stream waters that are derived from alpine areas, forested colluvial slopes, and near-channel wet areas (Dethier, 1988). Ideally, more frequent stream sampling could reduce the error imparted by uncertainties in long-term solute concentrations. Despite this, we are confident that the four sampling periods used to construct annual flux measures provides a reasonable estimate of the yearly variations in concentrations because: 1) our sampling periods covered the high and low flow portions of the hydrograph throughout the four seasons; 2) seasonal variations are reasonably small for dissolved Si which is used here as a measure of total silicate weathering rates; 3) catchment studies in the Oregon Cascades suggest that water residence time within a catchment is ~ 2 months and thus, short-duration storm events are likely to displace only a small fraction of stored water, generating a runoff chemistry that is dominated by old water with limited variability of runoff composition (Anderson and Dietrich, 2001); and 4) Cascade rivers generally show poor concentration/discharge correlations (Dethier, 1988).

Chemical Weathering Fluxes and Correction for Atmospheric Contributions

Chemical weathering fluxes were calculated by multiplying dissolved riverine cation concentrations for each sampling date by the calculated three-month discharge. Total annual dissolved fluxes were then calculated by summing the dissolved flux from all four sampling periods. Total chemical weathering fluxes and dissolved silica fluxes are calculated as follows: 1) three-month, $W_{\text{chem seasonal}} = C_{\text{Si}}Q_{\text{seasonal}} + C_{\text{Ca}}Q_{\text{seasonal}} + C_{\text{Mg}}Q_{\text{seasonal}} + C_{\text{Na}}Q_{\text{seasonal}} + C_{\text{K}}Q_{\text{seasonal}}$, where C is the concentration of individual solutes for a given sampling time and Q_{seasonal} is the three-month discharge, and $W_{\text{chem}} = \text{sum of all four three-month seasonal fluxes}$; and 2) $W_{\text{Si seasonal}} = C_{\text{Si}}Q_{\text{seasonal}}$ and W_{Si} is then summed for all three-month seasonal sampling periods.

Dry and wet atmospheric deposition of solutes can contribute a significant amount of cations and anions to a catchment. As a result, accurate estimates of the total flux of solutes from the weathering of silicate rocks requires correction for atmospheric deposition. We corrected for this using measured values collected from the North Cascades National Park Marblemount Ranger station (WA19), which is located ~ 50 km to the north of the Skykomish River basin. Direct monthly atmospheric deposition has been measured at this site over a period of fourteen years, including the 2003 to 2004 period of sample collection. Atmospheric contributions of Ca^{2+} , Mg^{2+} and K^+ are roughly constant over the fourteen year record of deposition and account for ~ 15 mol Ca ha^{-1} , 9 mol Mg ha^{-1} , and 4.5 mol K ha^{-1} per year on average. As a result, major cation fluxes are corrected for atmospheric deposition by subtracting the yearly totals (mol ha^{-1}) for the 2003 to 2004 period of stream sampling from each basin. However, over the fourteen year record of atmospheric deposition

measurements, total annual atmospheric contribution of sodium is directly proportional to the annual rainfall and follows the empirical relationship $\text{Na} \text{ (mol ha}^{-1} \text{ yr}^{-1}) = 0.87 \times \text{precipitation (cm)} - 66.5$. To correct our measured Na fluxes for atmospheric additions, we used the basin average annual precipitation and this empirical relationship. With the exception of Na, these additions comprise at most a few percent of the total annual elemental flux for each basin. No correction was made for atmospheric contributions of Si, as atmospheric contributions of this are generally very low. Si and major cation fluxes are given in table 2.

W_{chem} provides a measure of the total rate of chemical weathering and is a useful tool for understanding the coupling of chemical and physical denudation. However, we are primarily interested in the chemical flux derived only from the weathering of silicate minerals because over geologic time, the weathering of Ca- and Mg-silicates contributes to the long-term consumption of atmospheric CO_2 when coupled with carbonate precipitation in the oceans (Urey, 1952). Dissolved Si fluxes are not affected by the weathering of carbonate minerals and are therefore, useful as a measure of silicate weathering rates in terrains with mixed lithologies (Edmond and Huh, 1997; Waldbauer and Chamberlain, 2005). K^+ and Na^+ concentrations can also be a measure of silicate weathering rates, however we did not use these cations in our calculations because K^+ concentrations are relatively low and show a wide seasonal variability and Na^+ concentrations in these streams are strongly influenced by atmospheric deposition (up to 25%). In addition, we were unable to assign silicate weathering fluxes to specific silicate minerals such as plagioclase and biotite, as has been done in other studies (Jacobson and others, 2003). This is due to the fact that the bedrock in the Skykomish basin contains minor amounts of pyroxene- and Ca/Na-amphibole-bearing amphibolites which when weathered change the Ca/Na ratio of stream waters, and this ratio is used to determine the role of plagioclase weathering (Jacobson and others, 2003).

Total chemical weathering fluxes (W_{chem}) from the twelve catchments are universally high, ranging from $\sim 5100 \text{ mol ha}^{-1} \text{ yr}^{-1}$ to greater than $8800 \text{ mol ha}^{-1} \text{ yr}^{-1}$ (table 2). However, there is no apparent relationship between total weathering flux and catchment average exhumation rate, elevation, depth to bedrock, and/or temperature. Surprisingly, W_{chem} has a weak negative correlation with basin mean precipitation that is counter to the results of a number of studies that show that runoff is the dominant control on weathering fluxes (Dunne, 1978; White and Blum, 1995). Moreover, the large scatter of total chemical weathering rates (W_{chem}) observed within the Skykomish catchment is largely controlled by the Ca^{2+} and Mg^{2+} concentrations (table 1), which vary widely between individual streams.

In the twelve tributaries, dissolved Si fluxes range from ~ 1900 to $3000 \text{ mol ha}^{-1} \text{ yr}^{-1}$ with the highest fluxes occurring in the region of highest tectonic uplift/long-term erosion (table 2; fig. 5). Annual dissolved Si fluxes ($\text{mol ha}^{-1} \text{ yr}^{-1}$) show a general increase with distance eastward (fig. 5B; relative to a UTM easting of 504645 as used by Reiners and others, 2003) and weak or no correlation with basin mean precipitation, temperature, or elevation (figs. 5C, 5D, and 5E).

DISCUSSION

Climate, Exhumation, and Chemical Fluxes

Numerous studies show that temperature and precipitation are important regulators of chemical weathering rates (Velbel, 1993; Brady and Carrol, 1994; White and Blum, 1995; Gaillardet and others, 1999; Oliva and others, 2003). However, W_{chem} and W_{Si} show no clear relationship with temperature and both appear to exhibit no or a weak negative correlation with precipitation. With respect to W_{chem} , this may be due in part to the weathering of trace amounts of carbonate minerals in the catchment. This

can impact dissolved cation fluxes due to the fact that the dissolution rate of carbonate is several orders of magnitude greater than plagioclase (Chou and others, 1989; Blum and Stillings, 1995). This has been shown to be a significant source of dissolved Ca^{2+} and Mg^{2+} in other studies of tectonically active weathering environments (Blum and others, 1998; Jacobson and others, 2003) and in studies of the Washington Cascades (Dethier, 1986; Drever and Hurcomb, 1986; Dethier, 1988). However in general, the lack of correlation between climatic parameters and W_{chem} or W_{Si} , suggests that a number of factors may mask or overprint climatic effects on dissolved chemical fluxes in the Skykomish catchment. Several possible factors are: 1) the difference in basin averaged mean annual temperatures and precipitation in this study area is not large enough to generate significant measurable differences in chemical weathering rates; 2) dissolution of trace carbonates throughout the basins may have a strong impact on measured Ca^{2+} and Mg^{2+} fluxes and thus mask climatic signals in weathering fluxes; or 3) variations in erosion/exhumation rates across the studied catchment exert greater control over chemical weathering rates in this area than climatic variables, which has the effect of masking temperature or precipitation effects on dissolved weathering fluxes. Indeed, dissolved Si fluxes from the Skykomish are correlated with long-term basin erosion rates ($R^2 = 0.67$; excluding outlier MH-17). This agrees with a number of datasets that show that silicate weathering rates are strongly controlled by exhumation rate (Gaillardet and others, 1999; Riebe and others, 2001a, 2001b; Millot and others, 2002; Riebe and others, 2004a) and are proportional to the rate of supply of rock in transport-limited weathering environments, with climatic effects superimposed on tectonic or supply controls (West and others, 2005). Importantly however, one catchment (MH-17) exhibits particularly low dissolved Si fluxes despite high rates of erosion. This catchment is characterized by the highest rates of exhumation, high mean elevation, and cold temperatures. However, portions of this basin may be underlain by quartz-rich sandstone, which could account for the generally low rates of silicate weathering in this drainage.

Steady-state weathering models (Waldbauer and Chamberlain, 2005) suggest that the depth of the zone of weathering and the rate of rock uplift are important predictors of silicate weathering fluxes. While climatic parameters do not exhibit clear relationships with total chemical weathering fluxes or total dissolved Si fluxes, temperature, precipitation, and the rate of erosion all show weak relationships with the depth to bedrock in the study catchments. Calculated depth to bedrock is most correlated ($R^2 = 0.41$) with basin mean annual temperatures, and basins with higher temperatures exhibit the highest mean basin depths. Several factors may account for this relationship. First, catchments with lower mean elevations tend to have less area covered by steep-slopes and exposed bedrock and are thus more likely to be characterized as zones of sediment accumulation. Second, temperature is an important factor in biological productivity and thus plays an important role in the rate of generation of organic material. Finally, laboratory-weathering studies show the temperature dependence of mineral dissolution rate constants by an Arrhenius equation:

$$k = k_0 \exp\left(\frac{-E_a}{RT}\right) \quad (1)$$

where k is the rate constant, k_0 is the preexponential factor, and E_a is the apparent activation energy of dissolution. Thus, higher temperatures can influence mineral dissolution rates in the field and the rate of formation of weathering products.

In contrast with weathering zone depth and temperature relationships, basin mean depth to bedrock shows a weak negative or no correlation ($R^2 = 0.33$) with mean annual basin precipitation and long-term exhumation rate ($R^2 = 0.27$). This may be due to the fact that high elevation sites with steep slopes and high precipitation are also generally characterized by lower temperatures and subject to more frequent landslides

than lower elevation sites. However, scatter in the data makes it difficult to determine more specifically the link between precipitation, temperature, and erosion rates and depth to bedrock in these areas.

Steady State Chemical Weathering in the Washington Cascades

We undertook this study to explore the concept of steady-state chemical weathering in an area that has been proposed to be in physical steady state (Reiners and others, 2003). Specifically, we apply dissolved Si flux data from the Skykomish basin in concert with estimates of basin depth to bedrock and long-term exhumation rates to calibrate and test a model of steady-state weathering on a landscape scale (Waldbauer and Chamberlain, 2005). This model is described in detail below. Separation of two key variables in this model (weathering zone depth and uplift rate) allows us to quantitatively define supply- and reaction-limited weathering regimes and show that chemical weathering rates in the western Washington Cascades are controlled primarily by differences in the rate of rock supply with climatic controls (through partial regulation of weathering zone depth and kinetic rate constants), superimposed on this.

Although our first-order interpretation suggests that steady-state chemical weathering provides a reasonable approximation of observed chemical fluxes in the Skykomish basin, we realize that there are several potential flaws in this interpretation. First, whether or not a landscape is in chemical steady state, or for that matter, physical steady state, is at best, difficult to prove. Certainly there are both spatial (see for example Green and others, 2006) and temporal scales at which the concept of steady-state chemical weathering does not apply. For example, a direct comparison of weathering fluxes based on measurements of riverine chemistry could reflect processes that occur on very different timescales than long-term exhumation rates. Chemical fluxes measured from rivers may record processes that occur over timescales from 1 to 10^4 years such as logging, landslides and glaciation, whereas long-term exhumation measures record processes occurring over millions of years. Indeed, the Skykomish catchment was affected by alpine glacier erosion during the Quaternary and large-scale glaciation of the Cascade Range is thought to play a significant role in controlling the topographic and exhumation history of this range over the past million years (Mitchell and Montgomery, 2006). Work by Anderson (2005) demonstrates that glaciers show a direct linkage between erosion rate and chemical weathering fluxes as a result of the production of large volumes of weatherable material with high surface area. Thus, it is possible that modern weathering fluxes in the Skykomish basin record transient weathering phenomena that is out of equilibrium with the long-term glacial climate and exhumation history of the Skykomish catchment. However, dissolved Si fluxes correlate with (U-Th)/He measures of long-term erosion, which agrees with work by a number of authors who show that in large river basins and at the orogen scale, weathering rates correlate with long-term tectonic uplift/erosion and the residence time of rock in a zone of weathering (Jacobson and others, 2003; Waldbauer and Chamberlain, 2005; Chamberlain and others, 2005). This is likely because most riverine weathering flux measurements average weathering rates over an entire catchment, which can minimize the effect of local disturbances on overall weathering fluxes. Second, chemical steady-state and physical steady-state do not have to be linked. Numerical models suggest that physical steady-state in active mountain belts may occur over millions of years (Willet and others, 2001), whereas chemical steady-state, which may be defined as a state in which the rate of generation of product with respect to the introduction of reactant to the weathering system is constant on a basin-scale, is likely to be achieved at far shorter time-scales. However at present, the time-scales for reaching chemical steady-state are unknown. Given these caveats we examine how the steady-state chemical weathering model of Waldbauer and Chamberlain (2005) applies to the Skykomish basin.

Waldbauer and Chamberlain (2005) provide a model for examining the chemical flux from a landscape in which the residence time of material within the zone of active weathering is a key control of overall chemical weathering rates. In this model, rock uplift is balanced by the combined rate of chemical and physical erosion. For a system in both physical and chemical equilibrium within the weathering zone (residence time in the weathering zone $\tau = Z U^{-1}$), the flux of the weathered product from the landscape (F_{pi} [$\text{mol m}^{-2}\text{s}^{-1}$]) is described by:

$$F_{pi} = r_i U q_{oi} \left[1 - \exp\left(-\frac{A_i k_i}{U} Z\right) \right] \quad (2)$$

where r_i is the ratio of product to reactant (determined by reaction stoichiometry), q_{oi} is the concentration of the reactant mineral in unweathered bedrock, U is the rate at which fresh bedrock is moved into the weathering zone and is assumed equal to the rate of erosion (m s^{-1}), A_i ($\text{m}^2 \text{mol}^{-1}$) is the specific mineral surface area available to the chemical reaction, k_i ($\text{mol m}^{-2} \text{s}^{-1}$) is a kinetic rate constant, and Z (m) is the thickness of the active weathering zone and is assumed to be constant over time. To determine the total flux of an element of interest, equation 1 is summed over all mineral phases.

To examine the applicability of this model on the landscape scale in a region with climatic and tectonic gradients, we used the measured dissolved Si fluxes, spatially extrapolated (U-Th)/He-based basin exhumation rates, and spatially calculated depth to bedrock values (based on depth/slope relationship) for each of the twelve catchments as discussed above. The input parameters we used are as follows. First, in this model of chemical weathering we use a starting mineralogical composition similar to the Snoqualmie granodiorite [25% quartz, 10% orthoclase feldspar, 50% plagioclase feldspar ($\text{Ca}/(\text{Ca}+\text{Na}) = 0.37$), 8% hornblende, and 7% biotite; Erikson, 1969]. Second, because experimentally derived mineral dissolution rates are often two to four orders of magnitude faster than field-derived rates, we chose to treat individual mineral dissolution rates and surface areas as free parameters that must lie within the range of observed field-based rates. We chose initial A_i and k_i values within the mid-range of measured field values for granodioritic terrain. We then used the spatially extrapolated rate of rock uplift/exhumation and depth to bedrock at each 30 by 30 m area of the landscape to calculate the expected chemical flux ($\text{mol m}^{-2} \text{yr}^{-1}$) from the weathering of the Snoqualmie granodiorite and all its constituent minerals at each portion of the landscape. By summing the expected dissolved Si flux from all silicon-bearing mineral phases at each of these m^2 spots on the landscape, we calculated total catchment annual dissolved Si fluxes. A_i and k_i were then optimized for each Si-bearing mineral phase to reduce the misfit between observed and predicted catchment Si fluxes using a least-squares nonlinear inversion method (Dennis, 1977). This optimization required that each mineral dissolution rate for the field area must be in rough agreement with the Goldich weathering sequence (Goldich, 1938), which states that the general order of mineral weathering proceeds from the least stable to most stable minerals. The optimized rate constants (k_i) and surface areas (A_i) generated in this process fall in the middle of observed field mineral weathering rates for all minerals but quartz, which sits at the low end of field-measured dissolution rate (table 3).

Comparison of measured Si fluxes with predicted fluxes based on our optimized rate constants and surface area shows a good fit between observed and predicted fluxes ($R^2 = 0.64$; excluding outlier at MH-17) which attests to the general, if imperfect, ability of this weathering model in predicting Si fluxes on a landscape scale (fig. 6). Although climatic factors such as precipitation/runoff and temperature clearly affect chemical weathering rates (Velbel, 1993; White and Blum, 1995; Gaillardet and others,

TABLE 3
Granodiorite weathering model inputs

Mineral	Mineral Formula	Bedrock Composition (percent) ¹	Mineral Surface Area m ² mol ⁻¹	Density g cm ⁻³	Granodiorite (mol/m ³)	Log Dissolution Rate constant (mol m ⁻² s ⁻¹)	Reactive Surface Area (m ² mol ⁻¹)
Quartz	SiO ₂	25.0	2	2.65	11025	-18.0	1
Orthoclase	KAlSi ₃ O ₈	10.0	26	2.58	927	-15.0	12.5
Plagioclase	^{1,2} (Ca,Na) _{0.37} AlSi _{2.63} O ₈	50.0	108	2.70	5026	-14.0	82.5
Hornblende ³	Ca _{1.8} Mg _{1.9} Fe ₂ Al(Si ₇ Al)O ₂₂ (OH) ₂	8.0	493	3.00	282	-15.0	324.5
Biotite ³	KFe _{1.16} Mg _{1.3} Ti _{0.12} AlSi ₃ O ₁₀ (OH) ₂	7.0	1251	3.00	398	-14.0	2502

¹Average values for Snoqualmie Granodiorite from Tabor and Crowder (1969).

²Ca/Na_{plagioclase} ratios from Cloudy Pass Batholith.

³Cary, 1990.

1999; Oliva and others, 2003) and these parameters influence the depth to bedrock (fig. 4), in the Washington Cascades long-term exhumation/erosion is the best predictor of silicate mineral weathering fluxes. This conclusion is consistent with field studies (Riebe and others, 2001b) that show that in tectonically active areas, chemical weathering rates are more strongly controlled by rock erosion/exhumation than by climatic factors. That said however, one of the limitations to applying this model to different weathering environments is in the use of estimates of depth to bedrock within a landscape. As discussed previously, the depth of the zone in which active weathering occurs can be highly variable, ranging from centimeters to tens of meters in depth. In the absence of chemical analyses of drill cores, it is difficult to fully characterize the depth of the zone generating chemical fluxes in our model of depth to bedrock. In spite of this limitation, we show that we are broadly able to predict weathering fluxes throughout the Skykomish catchment using the optimized rate constants, exhumation/erosion rates, and depth to bedrock estimates for this area (fig. 6). Thus, the strength of this model rests in its ability to capture broad relationships between weathering rates, tectonic uplift, and the depth of the zone of weathering.

Predictions and Implications of Weathering Model

There are two predictions that can be made from the steady-state chemical weathering model that we calibrated using data from the Skykomish catchment. First, it is possible to define areas of a landscape that are reaction-limited and supply-limited. In Waldbauer and Chamberlain (2005) the effective surface age (τ) is a key determinant of the chemical flux from a landscape. This term encompasses both the rate of tectonic uplift and weathering zone depth within a single term that reflects the residence time of rock within a zone of weathering. However, combining these two terms into a single variable (τ) makes it difficult to examine how variations in one of these two parameters influences chemical fluxes at the extremes of low and high rates of tectonic uplift. Separation of these two terms allows us to place quantitative bounds on transport-limited and weathering-limited erosional regimes (Kirkby, 1971; Stallard and Edmond, 1983) and redefine them in terms of supply-limited and reaction-limited chemical weathering states (Hilley and others, unpublished data). By analyzing the time a given portion of rock remains within the weathering zone (ZU^{-1}) relative to the time-scale of the chemical weathering reaction process ($A_i^{-1}k_i^{-1}$), this model allows prediction of the flux of weathered product from a landscape. $A_i^{-1}k_i^{-1}$ can be thought of as a measure of the ratio of reactant to product (with units of time) and may be used to calculate the lifetime of a molar quantity of a reactant (for example the lifetime of a quartz grain). We define the ratio of these time-scales as $t^* = kAZ/U$. When the

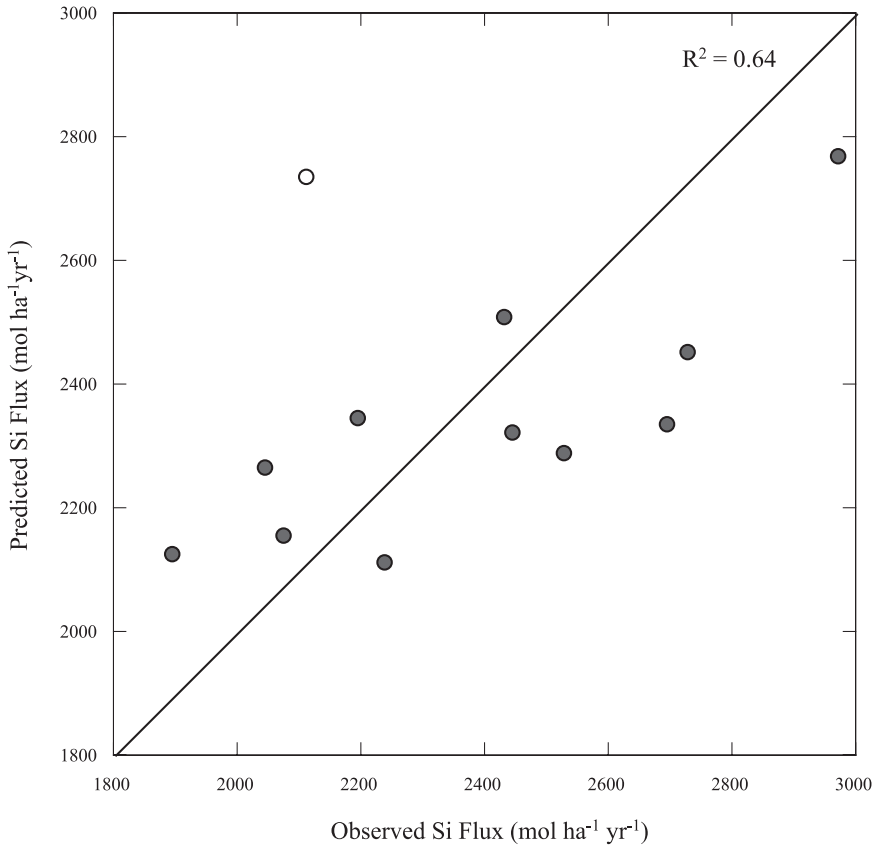


Fig. 6. Observed dissolved Si flux ($\text{mol ha}^{-1} \text{yr}^{-1}$) versus predicted dissolved Si flux from the calibrated steady-state chemical weathering model. Shown are the Si fluxes for the twelve catchments from the Skykomish River basin. The R^2 for the data is 0.67.

weathering reaction time-scale is much shorter than the residence time of rock in the soil column, $t^* \rightarrow 0$ and $F_{pi} = Zk_r A_i q_{or}$. Thus, for areas of a landscape dominated by thin weathering zones and rapid surface uplift or erosion, the flux of weathering reaction products are limited by reaction kinetics, weathering zone thickness, and abundance of reactant mineral in the underlying bedrock. Hence, this state is defined as reaction-limited (Hilley and others, unpublished data). Conversely, when rock uplift/erosion rates are low and weathering zones are thick, $t^* \rightarrow \infty$ and $F_{pi} = Uq_{or}$. In this case, weathering fluxes are limited by the supply of fresh bedrock into the weathering zone and depend only on the tectonic/erosional conditions and bedrock composition of a given area. Thus, we refer to this condition as supply-limited (Hilley and others, unpublished data). Between these two end-member states, the flux of weathering products will be determined by those factors that regulate the supply of rock to the weathering zone and those that control the reaction kinetics (fig. 7).

Using the calibrated weathering model it is possible to constrain the Skykomish basin with respect to reaction- and supply-limitation. Our analysis suggests that the twelve catchments examined here lie within the transition zone between reaction-limited and supply-limited weathering regimes (fig. 7) despite the range of uplift/exhumation rates for this area. However, portions of a landscape may exist in supply- or

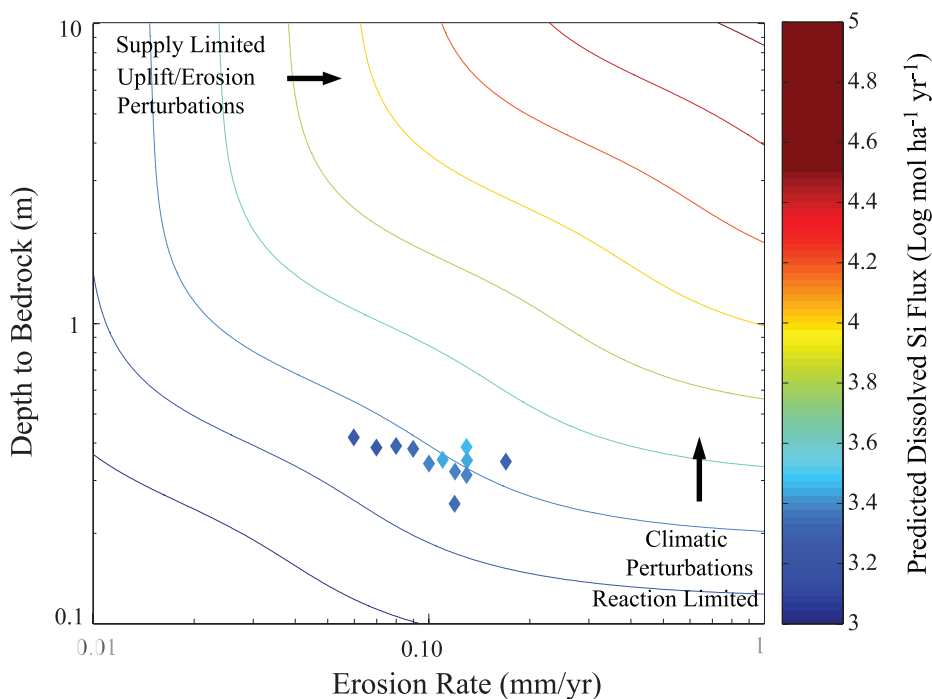


Fig. 7. Plot of the predicted log Si flux ($\text{mol ha}^{-1} \text{yr}^{-1}$) for the weathering of granodioritic terrains with a range of exhumation/erosion rates and weathering zone (depth to bedrock) thicknesses. A_i and k_i values from table 2 used. Colored lines indicate the expected log Si flux for a given exhumation/erosion rate and weathering zone depth. Colored diamonds represent weathering fluxes measured in this study from the central Cascades. Areas of high exhumation/erosion and thin weathering zones are characterized as reaction-limited and areas of low exhumation/erosion and thick weathering zones are characterized as supply-limited.

reaction-limited states. Areas of the Skykomish catchment with the highest rates of long-term exhumation/erosion ($>0.20 \text{ mm yr}^{-1}$) and thin weathering zones ($<1 \text{ m}$) are predicted to be close to a reaction-limited state because the supply of rock exceeds the ability of the system to chemically weather the rock. As a result, weathering fluxes from these areas may be affected by climatic perturbations such as temperature change or the development of strong precipitation gradients, while further increases in the rate of rock uplift or erosion in these areas may only result in increased rates of physical weathering and sediment storage. In contrast, areas with low rates of uplift/erosion and thick weathering zones ($>1 \text{ m}$) are predicted to be supply-limited and thus show exclusive weathering rate dependence on any changes in the rate of supply of weatherable material. Therefore, weathering rates in these areas of a landscape may be affected by sediment removal and increased erosion rates and less strongly impacted by climatic perturbations. Within the transition between these two states, weathering fluxes are expected to increase with increasing rates of rock supply and weathering zone depth.

Second, the model predictions have implications with regard to the role of weathering of Ca- and Mg-bearing silicate minerals on the regulation of CO_2 in the atmosphere, both at the landscape- and global-scale. Based on the Urey reaction (Urey, 1952), for every mole of Ca- or Mg-silicate mineral that weathers on the Earth's surface and forms Ca- or Mg-carbonate in the oceans, a mole of CO_2 is sequestered from the atmosphere. Using the Urey equation and equation 1 with the calibrated values of k_i , A_i

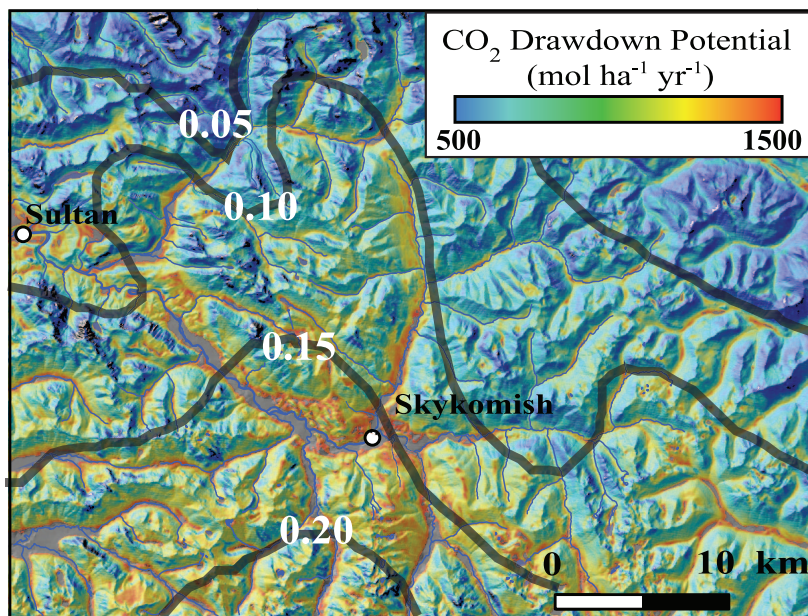


Fig. 8. Map of landscape-wide CO_2 consumption potential by silicate weathering across the Skykomish River catchment in the central Washington Cascades from predicted Mg^{2+} and Ca^{2+} fluxes from silicate weathering. Black shaded lines and white numerals show contours of the extrapolated erosion rates. High rates of erosion in the southern portion of the map result in strong tectonic control of net CO_2 consumption potential in this landscape. Short wavelength weathering zone depth effects result in elevated CO_2 consumption potential in valley bottom portions of the map.

and the appropriate stoichiometry for the silicate weathering reactions, we can use our spatially extrapolated rock uplift/erosion rate and weathering zone thicknesses across the Skykomish watershed to calculate the flux of individual elements such as Si, Ca^{2+} and Mg^{2+} from the weathering of the minerals that comprise granodiorite. This can then be used to predict the spatial distribution of the flux of Ca^{2+} and Mg^{2+} from silicate mineral dissolution. This calculated flux provides an estimate of the potential for net atmospheric CO_2 consumption by silicate weathering in the basin (fig. 8). Importantly, this calculation of potential CO_2 drawdown assumes that all Ca^{2+} and Mg^{2+} released from the weathering of silicates within the landscape is ultimately precipitated as carbonate in the ocean. Our calculations of net CO_2 drawdown potential over the watershed shows long-wavelength areas of CO_2 drawdown that result from increased rock uplift/erosion rates (fig. 8). However, a significant portion of the landscape also shows short-wavelength areas of CO_2 drawdown along valley bottoms that are related to changes in inferred weathering zone thickness.

While it is beyond the scope of this paper to map out predicted net CO_2 drawdown potential by silicate weathering globally, the calibrated model of silicate weathering and calculated net CO_2 drawdown plot of the Skykomish basin shows that silicate weathering rates and CO_2 consumption potential by weathering should vary dramatically on a landscape scale in response to varying erosional/tectonic conditions and weathering zone depths. Thus, an important inference that comes from this work is that chemical weathering rates in portions of a landscape dominated by low rates of uplift/erosion and thick weathering zones are governed by the supply of weatherable material. In contrast, chemical weathering rates in areas of a drainage with rapid rates of rock supply and relatively thin weathering zones are reaction-limited. In the first

case, the potential for any increase in net CO₂ consumption by weathering will depend upon only the rate of supply of weatherable material and the bedrock composition, whereas in the second, the CO₂ consumption potential will depend on reaction kinetics, bedrock composition, and weathering zone depth. If these regions are perturbed by any changes in climate and/or rock supply their weathering fluxes and resultant effect on the carbon cycle will change accordingly.

CONCLUSION

We measured Si and base cation fluxes from twelve catchments in the western Washington Cascades to examine the relationship between chemical weathering fluxes and long-term exhumation. We show that in this area, silicate weathering is strongly correlated with long-term exhumation rates and only weakly or not at all with climatic variables. We use measured Si flux data, estimated basin average depth to bedrock and long-term erosion rates to calibrate and test a steady-state chemical weathering model that emphasizes the role of tectonics in supplying rock to a zone of weathering. We show that separation of two key variables in this model: depth to bedrock (weathering zone depth) and uplift rate allows us to quantitatively evaluate the effects of tectonics and climate (through control of weathering zone depth) on chemical weathering in the Washington Cascades and as such, define weathering regimes that are reaction-limited and supply-limited. Changes in chemical weathering rates in these two weathering regimes will be through climate perturbations in tectonically active areas of a landscape or perturbations to the supply of fresh bedrock in regions of lower rates of uplift.

ACKNOWLEDGMENTS

We would like to thank Pete Reiners for supplying us with (U-Th)/He age data for this model and Mark Brandon for his AGE2Edot program to calculate erosion rates from these data. We are also grateful to Suzanne Anderson and an anonymous reviewer for a number of helpful critiques of this manuscript.

REFERENCES

- Anderson, S. P., 2005, Glaciers show direct linkage between erosion rate and chemical weathering fluxes: *Geomorphology*, v. 67, p. 147–157.
- Anderson, S. P., and Dietrich, W. E., 2001, Chemical weathering and runoff chemistry in a steep, headwater catchment: *Hydrological Processes*, v. 15, p. 1791–1815.
- Anderson, S. P., Dietrich, W. E., and Brimhall, G. H., 2002, Weathering profiles, mass-balance analysis, and rates of solute loss: Linkages between weathering and erosion in a small, steep catchment: *Geological Society of America Bulletin*, v. 114, p. 1143–1158.
- Berner, R. A., Lasaga, A. C., and Garrels, R. M., 1983, The carbonate-silicate geochemical cycle and its effect on atmospheric carbon dioxide over the last 100 million years: *American Journal of Science*, v. 183, p. 641–683.
- Blum, A. E., and Stillings L. L., 1995, Chemical weathering of feldspars, *in* White, A. F., and Brantley, S. L., editors, *Chemical Weathering Rates of Silicate Minerals*: Mineralogical Society of America, *Reviews in Mineralogy*, v. 31, p. 291–351.
- Blum, J. D., Gazis, C. A., Jacobson, A. D., and Chamberlain, C. P., 1998, Carbonate versus silicate weathering in the Raikhot watershed within the high Himalayan crystalline series: *Geology*, v. 26, p. 411–414.
- Brady, P. V., and Carroll, S. A., 1994, Direct effects of CO₂ and T on silicate weathering: Possible implications for climate control: *Geochimica et Cosmochimica Acta*, v. 58, p. 1853–1856.
- Brandon, M. T., Roden-Tice, M. K., and Garver, J. I., 1998, Late Cenozoic exhumation of the Cascadia accretionary wedge in the Olympic Mountains, NW Washington State: *Geological Society of America Bulletin*, v. 8, p. 985–1009.
- Cary, J. A., ms, 1990, Petrology and structure of the Lookout Mountain – Little Devil Peak area, North Cascades, Washington: Bellingham, Washington, Western Washington University, M.S. Thesis, 164 p.
- Chamberlain, C. P., Waldbauer, J. R., and Jacobson, A. D., 2005, Strontium, hydrothermal systems and steady-state chemical weathering in active mountain belts: *Earth and Planetary Science Letters*, v. 238, p. 351–366.
- Chou, L., Garrels R. M., and Wollast R., 1989, Comparative study of the kinetics and mechanisms of dissolution of carbonate minerals: *Chemical Geology*, v. 78, p. 269–282.
- Dennis, J. E. J., 1977, Nonlinear Least-Squares, *in* Jacobs, D., editor, *State of the Art in Numerical Analysis*: London, Academic Press, p. 269–312.
- Dethier, D. P., 1986, Weathering rates and the chemical flux from catchments in the Pacific Northwest,

- U.S.A., in Colman, S. M., and Dethier, D. P., editors, Rates of chemical weathering of rocks and minerals: New York, Academic Press, p. 503–530.
- 1988, A hydrogeochemical model for stream chemistry, Cascade Range, Washington, U.S.A.: *Earth Surface Processes and Landforms*, v. 13, p. 321–333.
- Drever, J. I., and Hurcomb, D. R., 1986, Neutralization of atmospheric acidity by chemical weathering in an alpine drainage basin in the North Cascade Mountains: *Geology*, v. 14, p. 221–224.
- Dunne, T., 1978, Rates of chemical denudation of silicate rocks in tropical catchments: *Nature*, v. 274, p. 244–246.
- Edmond, J. M., and Huh, Y., 1997, Chemical weathering yields from basement and orogenic terrains in hot and cold climates, in Ruddiman, W. F., editor, *Tectonic Uplift and Climate Change*: New York, Plenum Press, p. 329–351.
- Erikson, E. H., 1969, Petrology of the composite Snoqualmie batholith, Central Cascade mountains, Washington: *Geological Society of America Bulletin*, v. 80, p. 2213–2236.
- Gaillardet, J., Dupré, B., Louvat, P., and Allegre, C. J., 1999, Global silicate weathering and CO₂ consumption rates deduced from the chemistry of large rivers: *Chemical Geology*, v. 159, p. 3–30.
- Goldich, S. S., 1938, A Study in Rock Weathering: *Journal of Geology*, v. 46, p. 17–58.
- Green, E. G., Dietrich, W. E., and Banfield, J. F., 2006, Quantification of chemical weathering rates across an actively eroding hillslope: *Earth and Planetary Science Letters*, v. 242, p. 155–169.
- Heimsath, A. M., Dietrich, W. E., Nishizumi, K., and Finkel, R. C., 1997, The soil production function: *Nature*, v. 388, p. 358–361.
- Jacobson, A. D., Blum, J. D., Chamberlain, C. P., Craw, D., and Koons, P. O., 2003, Climatic and tectonic controls on chemical weathering in the New Zealand Southern Alps: *Geochimica et Cosmochimica Acta*, v. 67, p. 29–46.
- Kirkby, M. J., 1971, Hillslope process-response models based on the continuity equation: *Institute of British Geography Special Publication* 3, 15–30.
- Millot, R., Gaillardet, J., Dupré, B., and Allegre, C. J., 2002, The global control of silicate weathering rates and the coupling with physical erosion: new insights from rivers of the Canadian Shield: *Earth and Planetary Science Letters*, v. 196, p. 83–98.
- Mitchell, S. G., and Montgomery, D. R., 2006, Influence of a glacial buzzsaw on the height and morphology of the Cascade Range in central Washington State, USA: *Quaternary Research*, v. 65, p. 96–107.
- Oliva, P., Viers, J., and Dupré, B., 2003, Chemical weathering in granitic environments: *Chemical Geology*, v. 202, p. 225–256.
- Raymo, M. E., and Ruddiman, W. F., 1992, Tectonic forcing of late Cenozoic climate: *Nature*, v. 10, p. 117–122.
- Raymo, M. E., Ruddiman, W. E., and Froelich, P. N., 1988, Influence of late Cenozoic mountain building on ocean geochemical cycles: *Geology*, v. 16, p. 649–653.
- Reiners, P. W., Ehlers, T. A., Garver, J. I., Mitchell, S. G., Montgomery, D. R., Vance, J. A., and Nicolescu, S., 2002, Late Miocene exhumation and uplift of the Washington Cascades: *Geology*, v. 30, p. 767–770.
- Reiners, P. W., Ehlers, T. A., Mitchell, S. G., and Montgomery, D. R., 2003, Coupled spatial variation in precipitation and long-term erosion rates across the Washington Cascades: *Nature*, v. 426, p. 645–647.
- Riebe, C. S., Kirchner, J. W., Granger, D. E., and Finkel, R. C., 2001a, Minimal climatic control on erosion rates in the Sierra Nevada, California: *Geology*, v. 29, p. 447–450.
- 2001b, Strong tectonic and weak climatic control of long-term chemical weathering rates: *Geology*, v. 29, p. 511–514.
- Riebe, C. S., Kirchner, J. W., and Finkel, R. C., 2003, Long-term rates of chemical weathering and physical erosion from cosmogenic nuclides and geochemical mass balance: *Geochimica et Cosmochimica Acta*, v. 22, p. 4411–4427.
- 2004a, Sharp decrease in long-term chemical weathering rates along an altitudinal transect: *Earth and Planetary Science Letters*, v. 218, p. 421–434.
- 2004b, Erosional and climatic effects on long term chemical weathering rates in granitic landscapes spanning diverse climate regimes: *Earth and Planetary Science Letters*, v. 224, p. 547–562.
- Soil survey of Snohomish County area, Washington, 1983: *The Natural Resources Conservation Service*, v. 197, 62 p.
- Stallard, R. F., and Edmond, J. M., 1983, Geochemistry of the Amazon 2. The influence of geology and weathering environment on the dissolved load: *Journal of Geophysical Research*, v. 88, p. 9671–9688.
- Tabor, R. W., and Crowder, D. F., 1969, On batholiths and volcanoes – intrusion and eruption of Late Cenozoic magmas in the Glacier Peak area, North Cascades, Washington: *United States Geological Survey Professional Paper* 67, 60 p.
- Tabor, R. W., Frizzell, V. A., Booth, D. B., Waitt, R. B., Whetten, J. T., and Zartman, R. E., 1993, *Geologic Map of the Skykomish River 30'-by 60' Quadrangle*, Washington: U.S. Geological Survey Miscellaneous Investigations Map I-1963.
- Tangborn, W. V., and Rasmussen, L. A., 1976, Hydrology of the North Cascades region, Washington 2. A proposed hydrometeorological streamflow prediction method: *Water Resources Research*, v. 12, p. 203–216.
- Urey, H. C., 1952, *The planets: Their origin and development*: New Haven, Connecticut, Yale University Press, 245 p.
- Velbel, M. A., 1993, Temperature dependence of silicate weathering in nature: How strong a negative feedback on long-term accumulation of atmospheric CO₂ and global greenhouse warming?: *Geology*, v. 21, p. 1059–1062.
- Waldbauer, J. R., and Chamberlain, C. P., 2005, Influence of uplift, weathering and base cation supply on past and future CO₂ levels, in Ehleringer, J. R., Cerling, T. E., and Dearing, M. D., editors, *A history of*

- atmospheric CO₂ and its effects on plants, animals and ecosystems: Berlin, Springer Verlag, Ecological Studies, v. 177, p. 166–184.
- West, A. J., Galy, A., and Bickle, M., 2005, Tectonic and climatic controls on silicate weathering: Earth and Planetary Science Letters, v. 235, p. 211–228.
- White, A. F., and Blum, A. E., 1995, Effects of climate on chemical weathering in watersheds: Geochimica et Cosmochimica Acta, v. 59, p. 1729–1747.
- White, A. F., Blum, A. E., Schulz, M. S., Vivit, D. V., and Stonestrom, D. A., 1998, Chemical weathering in a tropical watershed, Luquillo mountains, Puerto Rico: I. Long-term versus short-term weathering fluxes: Geochimica et Cosmochimica Acta, v. 62, p. 209–226.
- Willet, S. D., Slingerland, R., and Hovius, N., 2001, Uplift, shortening, and steady-state topography in active mountain belts: American Journal of Science, v. 301, p. 455–485.